PNAS

Supplementary Information for

INSULIN REGULATES NEURO-VASCULAR COUPLING THROUGH ASTROCYTES

Ana M. Fernandez[1,2], Laura Martinez-Rachadell[1,2], Marta Navarrete[1], Julia Pose-Utrilla[2,3], Jose Carlos Davila[2,4], Jaime Pignatelli[1,2], Sonia Diaz-Pacheco[1], Santiago Guerra-Cantera[1,2], Emilia Viedma-Moreno[1,2], Rocio Palenzuela[5], Samuel Ruiz de Martin Esteban[5], Ricardo Mostany[6], Cristina Garcia-Caceres[7], Matthias Tschöp[7], Teresa Iglesias[2,3], Maria L. de Ceballos[1], Antonia Gutierrez[2,4], and Ignacio Torres Aleman[2,8,9,*]

*Correspondence to: Ignacio Torres Aleman

Email: ignacio.torres@achucarro.org

This PDF file includes:

Supplementary text
Figures S1 to S7
SI References

Materials and Methods

Animals: Wild type 6 months-old male mice (C57BL6/J) were used in EM experiments. Mice with insulin receptors ablated in GFAP (GFAP IR KO mice) or GLAST astrocytes (GLAST-IR KO mice) under regulation of tamoxifen were generated as described in detail before [1], by crossing hGFAP-CreER^{T2} or GLAST-CreER^{T2} on a C57 BL/6J background (FM Vaccarino, Yale Univ) with IR$^{f/f}$ mice having the IR gene flanked by loxP sites (R Kahn, Joslin Diabetes Center). Mice with IGF-I receptors ablated in GFAP astrocytes under the regulation of tamoxifen were obtained by crossingIGF-IR$^{f/f}$ mice (B6, 129 background; Jackson Labs; stock number: 012251) with CreERT2.GFAP mice (C57B&/6xSJL/J mix background; Jackson Labs, stock number: 012849, see [2] for further details). Intraperitoneal injection of tamoxifen for 5 consecutive days (75 mg/kg) to young mice (4-5 weeks old) eliminated IR or IGF-IR specifically in astrocytes, as reported [1]. Controls received vehicle injections (corn oil).

After tamoxifen injection, GFAP-IR KO mice showed significantly decreased levels of IR in brain, as compared to controls injected with the vehicle, regardless of the age at which they were injected and brain IR levels determined (Figure S1A,E,F). A group of control IR$^{f/f}$ mice received Tamoxifen injections and maintained intact responses to insulin (Figure S1D), demonstrating that tamoxifen has no impact on the phenotype, as already reported[1].GFAP/GLAST IR KO mice were genotyped using PCR protocols already detailed [1]. Multiplex PCR for GFAP IGF-IR KO genotyping included a common forward primer (P3, 5'−CTG TTT ACC ATG GCT GAG ATC TC−3') and two reverse primers specific for the wild-type (P4, 5'−CCA AGG ATA TAA CAG ACA CCA TT−3') and mutant (P2, 5'-CGC CTC CCC TAC CCG GTA GAA TTC-3') alleles. Mice had access to food and water *ad libitum* and were kept under light/dark conditions. Animal procedures followed European (86/609/EEC & 2003/65/EC, European Council Directives) guidelines and studies wereapproved by the respective local Bioethics Committees (Government of the Communityof Madrid, PROEX 193.4/20). Animals were not randomly assigned to the different experimental groups. Experimenters were not blinded to the procedures, except when indicated. GFAP IR KO mice and their control littermates were divided in young (<6 months old) and aged (>6 months old).

Reagents: The following reagents were used: N-acetyl-cysteine (NAC; Sigma, Darmstadt, Germany), Cyclosporine A (Sigma C1832), IGF-1 (PreproTech, Rocky Hill, NJ, USA), Insulin (Sigma), JC-1 (Invitrogen, Waltham, MA, USA), tomato lectin-FITC (Sigma), Tamoxifen (Sigma). Antibodies used were: ß-actin (Sigma cat. no. A5316), AKT (Cell Signaling Technology, Biotechnology, Dallas, TX, USA, cat. no. 2920), CD31 (Bioss antibodies, Woburn, MA, USA. cat. no. bs-0468R), Digoxigenin (Roche Diagnostics, Mannheim, Germany, cat. no.11333062910), Fis-1 (Proteintech, Rosemont, IL, USA, cat. no. 10956-1-AP), GFAP (Dako, Glostrup, DK, cat. no. Z0334), GluT1 (Invitrogen cat. no. PA1-46152), HIF1α (Cell Signaling Technology, cat. no. 36169), IGF-1 receptor ß (Cell Signaling Technology, cat. no. 9750), Insulin receptor ß (Santa Cruz cat. no. 23413), MAG (Abcam, Cambridge, USA cat. no. ab277535), MondoA (Invitrogen cat. no. PA5-41146), NeuN (Proteintech, cat. no. 26975-1-AP), MFN2 (Sigma cat. no. WH0009927M3), PGC1α (Millipore, Darmstadt, Germany, cat. no. AB3242), phospho-AKT (Cell Signaling Technology cat. no. 9271), phospho-tyrosine (pTyr, clone PY20, BD Transduction laboratories, San Jose, CA, USA, cat. no. 610000), PLP1 (Invitrogen cat. no. MA1-80034), TRPA1 (Invitrogen cat. no. OST00061W), and VEGF (Santa Cruz cat. no. sc-7269). Antibodies for proximity ligation assays included two pairs: VDAC1/Porin mouse monoclonal from Abcam (ab14734)- Grp75/MOT rabbit polyclonal (Abcam ab227215), and P3R-I/II/III mouse monoclonal from Sta Cruz (sc-377518)-Grp75/MOT rabbit polyclonal. Hoechst 33342 (DAPI) was purchased from Invitrogen.

Ca^{2+} imaging: Chronic glass-covered cranial windows were implanted at least 2 weeks before the beginning of the in vivo calcium imaging of astrocytes (Figure 2A). Briefly, mice were anesthetized (isoflurane, 5% for induction, 1.5% for maintenance via nose cone) and placed on a stereotaxic frame. Dexamethasone (0.2 mg/kg) and carprofen (5 mg/kg) were administered. A 4 mm-diameter craniotomy was performed with a pneumatic dental drill over the somatosensory cortex. A stereotaxic microinjection (400 nl; 30 nl/min) of AAV2/5-P_{GFAP}-Lck-GCaMP6f (PENN Vector Core; viral titer 6.13 x 10^{13}) was made. A round glass coverslip (5 mm) was laid over the dura mater, covering the exposed brain and part of the skull and glued to the latter with cyanoacrylate-based glue. A layer of dental acrylic was then applied throughout the skull surface and up to the

edges of the coverslip. A titanium bar (9.5 × 3.2 × 1.1 mm) was embedded in the dental acrylic to secure the mouse onto the stage of the microscope for imaging.
Imaging of GCaMP6f-expressing astrocytes was performed with a two-photon laser scanning microscope, custom-modified with a femtosecond laser (Chameleon Ultra II, Coherent Inc) and ScanImage 3.8 software written in MATLAB (MathWorks; RRID:SCR_001622), under isoflurane anesthesia (1%–1.5%). Mice were secured to the microscope using the titanium head bar. A 10X immersion objective (numerical aperture, NA, of 0.45, Nikon) was used to create a map of the area of interest and a 40Xwater-immersion objective (NA=1.1) was used for visualization of individual areas.
Excitation of GFP was achieved by tuning the laser at 780 nm with a power at the sample of < 20mW. After two weeks of surgery and viral injection, specific expression of constructs in the astrocytes was confirmed by immunostaining. Images were acquired every 1.4-1.7 seconds and ROIs were designed with ImageJ in a semi-automated manner using the GECIquant program. Ca^{2+} variations were estimated as changes of the fluorescence signal over baseline ($\Delta F/F_0$), and regions of interest were considered to respond to the stimulation when $\Delta F/F_0$ increased three times the standard deviation of the baseline. The astrocyte Ca^{2+} signal was quantified from the Ca^{2+} oscillation frequency. The time of occurrence was considered at the onset of the Ca^{2+} spike. Custom-written software in MATLAB (MATLAB R2016; Mathworks, Natick, MA)was used for computation of fluorescence of each ROI.

Cell cultures and transfections: Cultures were done as previously described in detail [3]. For astroglial cultures, postnatal (day 3–4) brains from control and GFAP IR KO mice were dissected, cortex and hippocampus removed, and mechanically dissociated. The resulting cell suspension was centrifuged and plated in DMEM/F-12 (Life Technologies) with 10% fetal bovine serum (Life Technologies) and 100 mg/ml of antibiotic-antimycotic solution (Sigma-Aldrich, Spain). After 15–20 days, astrocytes were re-plated at 1.2×10^5 cells/well. To downregulate IR expression in astrocytes obtained from GFAP IR KO mice, OH-tamoxifen (1μM) or the vehicle were added and cultures were used after 48 h, when IR levels were reduced. Endothelial cell cultures were performed as described [4], with modifications [5]. Briefly, dissection was performed on ice and cortices were cut, and digested in a mixture of collagenase/dispase (270 U collagenase/ml, 0.1%

dispase) and DNAse (10 U/ml) in DMEM (Life Technologies) for 1.5 h at 37°C. The cell pellet was separated by centrifugation in 20% bovine serum albumin/DMEM (1000g, 15 min) and incubated in a collagenase/dispase mixture for 1 hat 37°C. Capillary fragments were retained on a 10µm nylon filter, removed from the filter with endothelial cell basal medium (Life Technologies), supplemented with 20% bovine plasma-derived serum and antibiotics (penicillin, 100 U/ml; streptomycin, 100 µg/ml), and seeded on dishes coated with collagen type IV (5 µg/cm^2) at 0.5×10^5 cells/well. 3µg/mL puromycin was added for 3 days. Puromycin was then removed from the culture medium and replaced by fibroblast growth factor (2 ng/ml) and hydrocortisone (500 ng/ml). For co-cultures of endothelial cells / astrocytes the cell density was the same as in single cultures (1:2.4 ratio). Experiments were done after 1 week in culture without serum.

For transfection, astrocytes were electroporated (2×10^6 astrocytes with 2 µg of plasmid DNA) before seeding using an astrocyte Nucleofector Kit (Amaxa, Lonza, Switzerland). After electroporation, cells were plated to obtain a final cell density on the day of the experiment similar to that obtained with the transfection method. The transfection efficiency was 60–80%, as assessed with a GFP vector expression.

Insulin administration: Mice were anesthetized with isofluorane with oxygen flux at 0.8–1 l/min. The common carotid artery was exposed, and the external carotid ligated. A guide cannula was inserted in the common carotid artery and 100µl of 30µg/ml Dig-insulin was injected as a bolus using a Hamilton syringe coupled to a nanoinjector. After 1 hour, mice were perfused with saline and 4% paraformaldehyde. Brains were removed and processed forimmunohistochemistry. We determined whether Digoxigenin-labelled insulin preserved biological activity by western blot analysis of Akt phosphorylation in the brain of control mice receiving 15 min before an intracarotid injection of Dig-ins or Dig only (as a control). Preserved activity was seen in both freshly prepared Dig-insulin or after 2 months of storage at -20ºC (Figure S2A). For IR phosphorylation experiments, mice were injected with 3IU insulin/Kg body weight intraperitoneally (100 µl, 1 hour) or intra-parenchyma (2 µl, 15 min). For the latter, a Hamilton micro-syringe was inserted in the left lateral somatosensorial cortex with the following coordinates: 1.7 mm posterior and 1 mm lateral relative to bregma (left hemisphere), and 0.8 mm down the skull surface. Mice were then perfused with 40 ml saline for 15 min followed by 50 ml 4%

paraformaldehyde for 25 min. Brain and skeletal muscle were isolated and frozen until assayed by IR immunoprecipitation and Western blot with anti-pTyr. For cultures, insulin was used at 1mg/ml, under serum-free conditions.

Digoxigenin-labeled insulin: 100 µl of 1 mg/ml recombinant human insulin (Sigma) was mixed with 1 ml of PBS pH 8.5. Digoxigenin-3-O-methylcarbonyl-ε-aminocaproicacid-N-hydroxysuccinimide ester (NHS-Dig; Roche Diagnostics) dissolved in dimethyl sulfoxide (DMSO) was added to the insulin solution at a molar ratio of 1:5. After incubation at room temperature for 2 h, non-reacted NHS-Dig was removed by a Sephadex G-25 column (GE Healthcare, Chicago, IL, USA). Digoxigenin-labeled insulin (Dig-insulin) was stored at -20°C until use.

Immunofluorescence: Immunolabeling was performed as described [6]. Mice were deeply anesthetized with pentobarbital (50 mg/kg), and extensively perfused trans-cardially with saline followed by 4% paraformaldehyde in 0.1 M phosphate buffer,pH 7.4 (PB) as in insulin administration section. Saline perfusion was intended to eliminate insulin binding to brain vessels. Brains were then dissected, and coronal 50-µm-thick brain sections were cut in a vibratome and collected in PB. Sections were incubated to block non-specific antibody binding, followed by incubation overnight at 4°C with the primary antibodies in PB - 1% bovine serum albumin - 1% Triton X-100 (PBT). After several washes in PBT, sections were incubated with the corresponding Alexa-coupled secondary antibody (1:1000, Molecular Probes, ThermoFisher Scientific) diluted in PBT. Again, three 5-minute washes in PBT were required. Slices were rinsed several times in PB, mounted with gerbatol mounting medium, and allowed to dry. For endothelial cell staining, sections were incubated with Tomato lectin-FITC overnight at 4ºC followed by several washes in PBT. Omission of primary antibodies was used as control. Confocal analysis was performed in a Leica microscope (Wetzlar, Germany).

Proximity ligation assays (PLA): Assays were run using the Duolink® In Situ Detection Reagents Red Kit (DUO92008, Merck) as described [7]. Brain slices were incubated with 1% Triton X-100 phosphate-buffered saline (PBS-T) filtered solution during 5 minutes, washed 3 times in PBS (5 min each wash) and incubated with filtered glycine 20mM/PBS 0.1M for 10 minutes at room temperature (RT). Thereafter, the solution was removed and slices placed over gelatin-coated microscope slides and 30 µl

of Duolink blocking solution (1X) were added per section and incubated 1 hour at 37ºC inside a pre-heated humidity chamber. Slices were then incubated overnight at 4ºC with pairs of primary antibodies: VDAC1/Porin mouse monoclonal antibody (1:50) and Grp75/MOT rabbit polyclonal antibody (1:100) or IP3R-I/II/III mouse monoclonal antibody (1:50) and Grp75/MOT rabbit polyclonal antibody, diluted in Duolink blocking solution (1x). Negative controls were treated only with anti-Grp75**.** The next day, slices were washed twice with buffer A and then incubated for 1 hour at 37ºC with Duolink secondary antibodies (PLA probes). Slices were again washed with buffer A solution (3X) at room temperature and incubated with a mixture of ligation buffer (1:5) and ligase (1:40), both diluted in DNAse-free water. The ligation reaction was left 30 minutes at 37ºC, and slices were then washed twice with buffer A, and the amplificationreaction performed. Then, sections were incubated for 100 minutes at 37ºC with a mixture of Duolink amplification buffer (1:5) and polymerase (1:80), both diluted in DNAse-free water. Two 10-minute washes with Buffer B were performed. Sections were fixed for 10 min at room temperature with 4% paraformaldehyde solution and washed 3 times in PBS. Thereafter, GFAP immunocytochemistry was performed. PLA puncta were scored using the Imaris software with images taken at 63X objective in a confocal microscope. For counting, a surface was created in the green channel (GFAP staining) to select all $GFAP^+$ cells. Next, 10µm diameter spots were created in the blue channel (DAPI stain) to select the nuclei on that surface, obtaining the total number of $GFAP^+$ cells. Finally, a second spot was created in the redchannel (1µm diameter) to select all the PLA points present on the previously created surface. The ratio of PLA points/$GFAP^+$ cell was then calculated.

Vessel density: Images were taken at 40X on a Leica confocal microscope from coronal sections (50µm) of mouse brain cortex. Using IMARIS 9.6.0 software, a 3D surface was created in the green channel thus selecting all vessels. The surface covers the entire thickness of the section. We selected "average values" in the control panel to obtain the data for the volume of the vessels (µm3). This volume corresponds to the 3D surface created and is directly proportional to the volume of vessels. Images were scored blinded.

NAC administration: 6-week-old control littermates and GFAF IR KO mice were provided given a 1% solution of N-acetyl-L-cysteine in the drinking water (pH 7.2;

Sigma) for a period of 4 months. Then, mice were submitted for SPECT and PET analysis. Later, mice were sacrificed and brain GSH content was measured.
For cell cultures, NAC was used at 10mM during 24h followed by different biochemical determinations

Quantitative PCR: Total RNA isolation from brain tissue was carried out with Trizol. One mg of RNA was reverse transcribed using High Capacity cDNA Reverse Transcription Kit (ThermoFisher Scientific, Waltham, MA, USA) according to the Manufacturer's instructions. For quantification of specific genes, total RNA was isolated and transcribed as above and 62.5 ng of cDNA was amplified using TaqMan probes for mouse IGF-1receptor (IGF-1R) and Insulin receptor (InsR), and rRNA 18S as endogenous control (ThermoFisher Scientific). Each sample was run in triplicate in 20 µL of reaction volume using TaqMan Universal PCR Master Mix according to the manufacturer's instructions (ThermoFisher Scientific). All reactions were performed ina 7500 Real Time PCR system (ThermoFisher Scientific). Quantitative real time PCR analysis was carried out as described[8]. Results were expressed as relative expression ratios on the basis of group means for target transcripts versus reference 18S transcript.At least five independent experiments were done.

Immunoprecipitation and Western blotting: Assays were performed as described [9]. Brain tissue was homogenized in ice-cold buffer with 10mM Tris HCl pH 7.5, 150mM NaCl, 1mM EDTA, 1mM EGTA, 1% Triton X-100, 0.5% NP40, 1mM sodium orthovanadate, and a protease inhibitor cocktail (Sigma) plus 2mM PMSF, using 1 ml of buffer per mg of tissue. Insoluble material was removed by centrifugation, and supernatants were incubated overnight at 4 ºC with the antibodies (5µg/ml). Immunocomplexes were collected with Protein A/G agarose (Santa Cruz Biotechnology) for 1 h at 4 °C, centrifuged at 10.000 rpm during 5 min and washed 3X in homogenization buffer before separation by SDS-polyacrylamide gel electrophoresis and transferred to nitrocellulose membranes. After blocking for 1 h with 5% BSA in TTBS (20 mM Tris-HCl, pH 7.4, 150 M NaCl, 0.1% Tween 20), membranes were incubated overnight at 4 ºC with the different antibodies in TTBS, washed, incubated with secondary antibodies and develop using the Odissey procedure(Li-Cor Biosciences, Lincoln, NE, USA).

Immunoelectron microscopy: Immunogold procedure was performed as previously described [10]**.** After deep anesthesia with sodium pentobarbital (60 mg/kg), 6 month-old male mice (C57BL6/J) were perfused transcardially with 0.1 M phosphate-buffered saline (PBS), pH 7.4 followed by fixative solution containing 4% paraformaldehyde, 75 mM lysine and10 mM sodium metaperiodate in 0.1 M PB, pH 7.4. Brains were removed, post-fixed overnight in the same fixative solution at 4°C, coronally sectioned at 50 μm thicknesses on a vibratome (Leica VT1000S), and serially collected in wells containing cold PB and 0.02% sodium azide. For IGF-1R or IR immunogold labelling, sections containing the somatosensory cortex were used. Sections were first washed with PBS and incubated in a 50 mM glycine solution 5 minutes to increase antibody binding efficiency. Following a standard immunohistochemical protocol, tissue was firstfree-floating incubated in a rabbit polyclonal anti-IGF-IRα antibody or a anti-IR antibody in a PBS 0.1M/1% BSA solution for 48 hours at 22ºC. Then, sections were washed in PBS, and incubated with 1.4 nm gold-conjugated goat anti-rabbit IgG (1:100;Nanoprobes) overnight at 22ºC. After post-fixing with 2% glutaraldehyde and washing with 50 mM sodium citrate, labelling was enhanced with the HQ Silver^{TM} Kit (Nanoprobes), and gold toned. Finally, immunogold labelled sections were fixed in 1% osmium tetroxide, block stained with uranyl acetate, dehydrated in acetone, and flat embedded in Araldite 502 (EMS, USA). Selected areas were cut in ultrathin sections (70-80 nm) and examined and photographed with a JEOL JEM1400 electron microscope. As a control for the immunogold technique, sections were processed as above but omitting the primary antibody. No specific labelling was observed in these control sections.

SPECT/CT Imaging: Mice were imaged by SPECT/CT at the Brain Imaging Unit of the Cajal Institute (CSIC). Animals were handled blinded. Awake mice were iv injectedwith ^{99m}Tc-HMPAO (exametazine, Curium Pharma, Madrid, Spain) via a catheter inserted in the tail vein, in a volume of 0.2 ml. An ISOMED 2010 dose calibrator (activity 20 interval 1 μCi-1350 mCi, in the case of ^{99}mTc) was used to calibrate radiotracer doses. Thirty minutes after the injection of the radiotracer (32-42 MBq), to allow its biodistribution, mice were anesthetized with isoflurane (4% induction, 2% maintenance) in O_2 (0.7 l/min). SPECT and CT images were acquired with a bimodal Albira SPECT/CT preclinical imaging system (Bruker). All SPECT acquisitions were made with

FOV of 40 mm, comprising the head, for 30 min, with a single-pinhole collimator, and 60 projections of 60 sec each. This was followed by a 10 min CT scan (quality Best, capture mode step & shoot, 600 projections, voltage 45 kV and intensity 400 µA). The SPECT/CT scans were reconstructed with OSEM algorithm (5 subsets, 2 iteractions) and FBO, respectively, with the Albira suite Reconstructor software (Bruker). SPECT and CT images were fused and analyzed using PMOD software version 3.3 (PMOD Technologies LLC, Switzerland). Activity was quantified by matching the CT image of the skull of each animal to a common magnetic resonance (MR) mouse brain template, in which regions of interest (ROI) were previously delineated, as described elsewhere [89]. After saving the spatial transformation, it was applied to the corresponding fused SPECT image, to allow the correct co-registration tothe MR brain template. ROI activity uptake was expressed as the percentage injected activity (%ID). Results are mean ± SEM.

^{18}F-FDG PET imaging: ^{18}F-FDG PET was used to measure brain glucose handling as described in detail before [11]. ^{18}F-FDG uptake in the different brain regions was calculated in kBq/cc units. Animals were handled blinded.

ROS imaging: Brain ROS levels were visualized following previously published procedures with some modifications [12]. Animals were handled blinded. Briefly, DHE (Dihydroethidium, D11347, Invitrogen) solution (1.25 mg/mL) was freshly prepared in anhydrous DMSO under low-flow nitrogen gas in the dark. Just before injection, DHE solution was mixed with an equal volume of sterile saline, and injected intraperitoneally in two doses of 20 mg/Kg separated by 30 min. After 18 h, mice were intracardially perfused with 4% PFA. The brains were removed and postfixed in 4% PFA. Following 24 h, images were acquired *ex vivo* with an IVIS Spectrum instrument (Xenogen) (excitation filter, 518 nm; emission filter, 605 nm; exposure time, 1 s; bin, 8; f/stop, 2). Image analysis was performed by drawing a ROI around the whole brain and recording the mean pixel intensity using IVIS Lumina software. Results were plotted as mean pixel intensities using GraphPad Prism 4 (La Jolla, CA, USA).

Biochemical assays: The NAPDH/NAPD ratio in astrocytes obtained from GFAP IR KO mice was calculated using a fluorometric NADP/NADPH assay (Abcam ab176724). ROS levels in sh-RNA transfected astrocytes was determined using the fluorescent H2DCFDA (Invitrogen D399) ROS indicator as described before [13]. GSH levels in GFAP

IR KO astrocytes were assessed using a fluorimetric glutathione assay (Sigma CS1020) according to the manufacturer's instructions. Fluorescence was measured using a fluorescence reader (FluorStar, BMG LabTech, Ortenberg, Germany).

JC-1 flow cytometry: Astrocytes were nucleofected with IR siRNA or a siRNA with a random sequence (siRNA scramble) as control and were grown in normal conditions for 3-4 days and then incubated for 5 minutes in the presence of JC1. Cells were washed and harvested with trypsin. JC1 staining was assayed by flow cytometry. Side scatter analysis and Propidium Iodide was used to discard death cells and gate selection.

Statistics: The sample size for each experiment was chosen based on previous experience and considering a reduced use of animals. No blinding of data was used, except when indicated. All data were included for analysis. Values were relativized compared to the control or baseline condition. When using replicated measurements, average values were calculated. Results are expressed as the average of the relative values obtained in each independent test (mean ± SEM) for each experiment. Data wereanalyzed with GraphPad Prism 8.0 software. Normality was verified using the Kolmogorov-Smirnov test. Student's t test was used for comparison of two groups, or 1-or 2- way ANOVA for comparison of more than two groups with a Bonferroni post-hocanalysis. For non-normally distributed data, we used the Kruskal-Wallis test followed by the Wilcoxon test. A statistically significant difference was considered when p value < 0.05.

Supplementary Figure 1: **A,** Brain IR levels are reduced in GFAP IR KO mice as compared to controls (oil-injected). Representative WB is shown (n=9; t-test, t= 3.63; **p<0.01). **B,** Intra-parenchymal injection of insulin (3 IU/2 µl) to GFAP IR KO mice stimulates tyrosine phosphorylation of IR (pTyr) to the same degree than vehicle-injected littermates (n=10). Representative blot and quantitation histogram. **C,** Systemic injection of IGF-I (1 µg/gr, ip) elicits Tyr phosphorylation of the IGF-I receptor in the brain of GFAP IR KO mice similar to vehicle-injected controls (n=10). Representative blot is shown. **D,** $IR^{f/f}$ mice injected with tamoxifen show preserved brain IR phosphorylation in response to systemic insulin. **E,** Representative WB showing lower brain IR levels in GFAP IR KO mice injected at 4-5 weeks of age with tamoxifen and maintained until 12 months of age, when IR levels were determined. **F,** Brain IR levels in GFAP IR KO mice injected at 11 months of age with tamoxifen and maintained until 12 months of age, when IR levels were determined.

Supplementary Figure 2: **A,** Control mice injected in the carotid artery 15 min before with Digoxigenin-labelled insulin (Dig-Ins) or Dig alone (as a control) show increased Akt phosphorylation in brain. Both freshly prepared (upper blot) Dig-Ins, or after 2 months storage at -20ºC (lower blots) show preserved biological activity. **B,** Brain vessels ensheathed with astrocytic end-feet (GFAP staining in green) do not show accumulation of Dig-ins (DIG, in red) after intracarotid injection in control GFAP-IR KO mice (oil injected, upper picture), while in mice lacking astrocytic IR after administration of tamoxifen (lower picture), DIG label is patent (n=10). **E,** mRNA levels of GluT-1 in brain of young GFAP IR KO (left histograms) or GLAST IR KO (lower histograms) mice is significantly decreased, whereas in adult GFAP IR KO mice GluT-1 mRNA levels are normalized (n=9; t-test, t= 3.43; ***p<0.001).

Supplementary Figure 3: **A**, Brain perfusion determined by brain ^{99m}Tc-HMPAO uptake did not change in control littermates along age. **B**, Brain perfusion was decreased in aged GFAP IR KO mice (1 year-old) as compared to young ones (n= 9; t-test, t= 3.02; *p<0.01). **C,** Brain perfusion remains normal in GFAP IR KO mice given tamoxifen at 1 year of age (n=9). **D,** Brain perfusion in GFAP IGF-IR KO mice is not altered as

compared to vehicle-injected controls (n=5-6 per group). **E-F,** ROS levels in the brain of young (E; n=11-10) GFAP-IR KO mice are increased as compared to controls, without reaching statistical significance (#p=0.055, two-tailed t-test), while adult GFAP-IR KO mice (F; n= 8-13) show no changes (p=0.88, two-tailed t-test). **G-H,** Brain glucose uptake determined by ^{18}F-FDG did not change along age in control littermates (G) whereas in GFAP IR KO mice showed a significant increase (H) (n= 8; t-test, t= 3.61 **p<0.01 vs respective control group). **I,** The MAG/PLP1 protein ratio determined by WB in brain tissue in young GFAP IR KO mice and their control littermates (control n=8, and tamoxifen n=5).

Supplementary Figure 4: **A,** Expression of TGFβ3, ErbB2, VEGFa and VEGFc was increased in young GFAP IR KO mice (n=10; t-test, t= 3.13, ***p<0.001 and *p<0.05). **B,** In older GFAP IR KO mice (>12 months), expression levels of TGFβ3, Errb2, and VEGFc were normal whereas VEGFa was significantly decreased (n=10; t-test, t= 3.76, *p< 0.05). **C, D,E,** Expression of angiogenic mediators MmP14 (D) and PTGS1 (E) is not altered in the brain of young GFAP IR KO mice (n=8).

Supplementary Figure 5: A-G, Brain mRNA levels of VEGFa (A), VEGFc (B), TGFβ3 (C), ErbB2 (D), vWF (E), Mmp14 (F), and PTGS1 (G) are significantly increased in GLAST IR KO mice as compared to control (vehicle-injected) littermates (n=7 per group; *p<0.05; **p<0.01 and ***p<0.0001).

Supplementary Figure 6: A, Insulin increases VEGF (upper panels, n= 9; t-test, t= 3.24; **p<0.01) and HIF1α levels in wt astrocytes (lower panels, n= 9; t-test, t= 3.21; **p<0.01). **B,** IR levels in astrocytes obtained from GFAP-IR KO mice and treated with OH-tamoxifen are decreased. Representative blot and quantitation bars are shown (**P<0.01). **C,** High glucose increases VEGF (left panels, n=9; 1-way ANOVA, F= 10.42; *p<0.05) and HIF1α levels in wt astrocytes (right panels, n= 9; 1-way ANOVA, F= 10.29; *p<0.05). Representative blots and quantitation histograms are shown.

Supplementary Figure 7: **A** Mitochondrial depolarization was determined by JC1 staining and flow cytometry. Upper plots: representative red versus green fluorescence scatter in siRNA scramble (left) and siRNA IR (right) nucleofected cells. Lower: representative histograms of cell counts and their red (left) or green JC1 fluorescence (right) intensity levels in siRNA scramble (grey line) and siRNA IR nucleofected astrocytes (black line) (n=8). **B-E,** Cyclosporine treatment of shIR astrocytes normalized the Mfn2/Fis1 ratio (B), and the levels of HIF1α (C), VEGF (D) and GluT1 (E) (n=9).

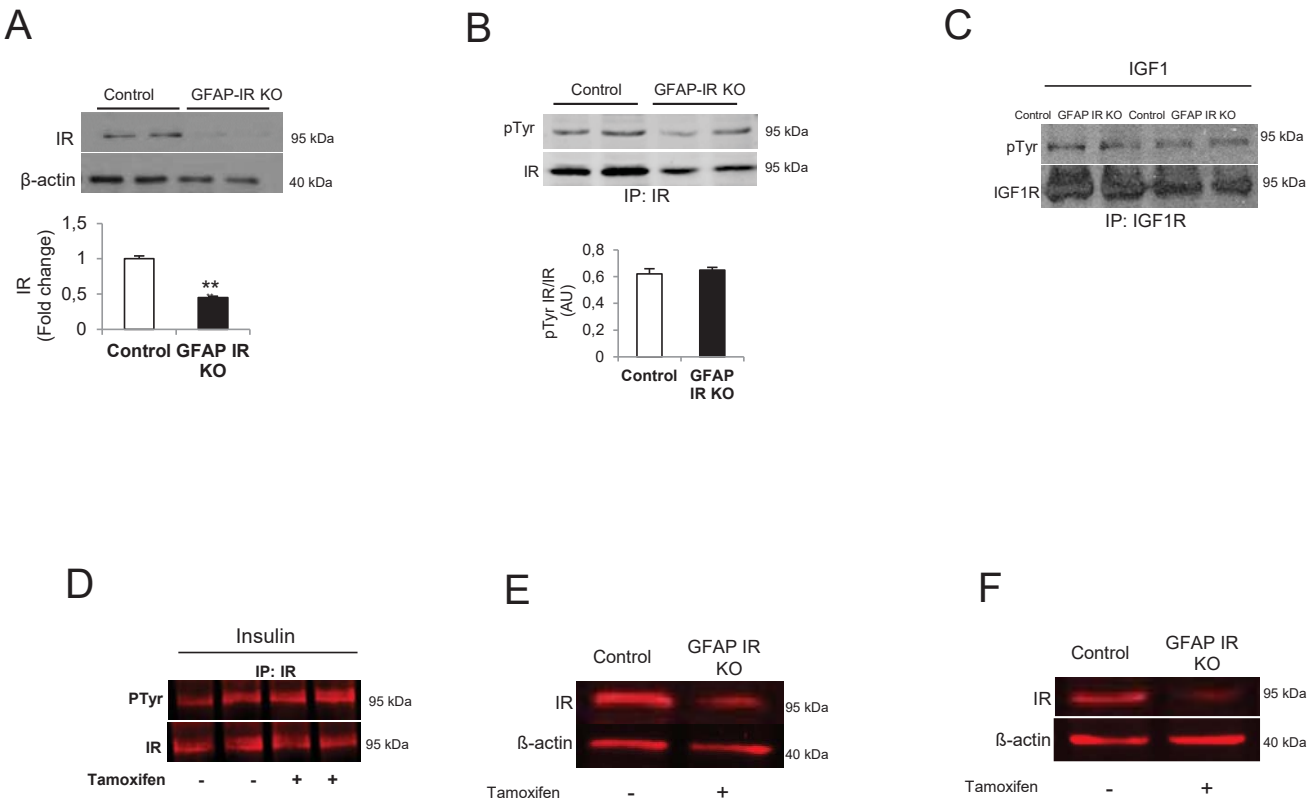
A
Control
GFAP-IR KO
IR
β-actin
95 kDa
40 kDa
IR (Fold change)
1,5
1
0,5
0
**
Control
GFAP IR KO
B
Control
GFAP-IR KO
pTyr
IR
95 kDa
95 kDa
IP: IR
pTyr IR/IR (AU)
0,8
0,6
0,4
0,2
0
Control
GFAP IR KO
C
IGF1
Control
GFAP IR KO
Control
GFAP IR KO
pTyr
IGF1R
95 kDa
95 kDa
IP: IGF1R
D
Insulin
IP: IR
PTyr
IR
95 kDa
95 kDa
Tamoxifen
-
-
+
+
E
Control
GFAP IR KO
IR
ß-actin
95 kDa
40 kDa
Tamoxifen
-
+
F
Control
GFAP IR KO
IR
ß-actin
95 kDa
40 kDa
Tamoxifen
-
+

Figure S1

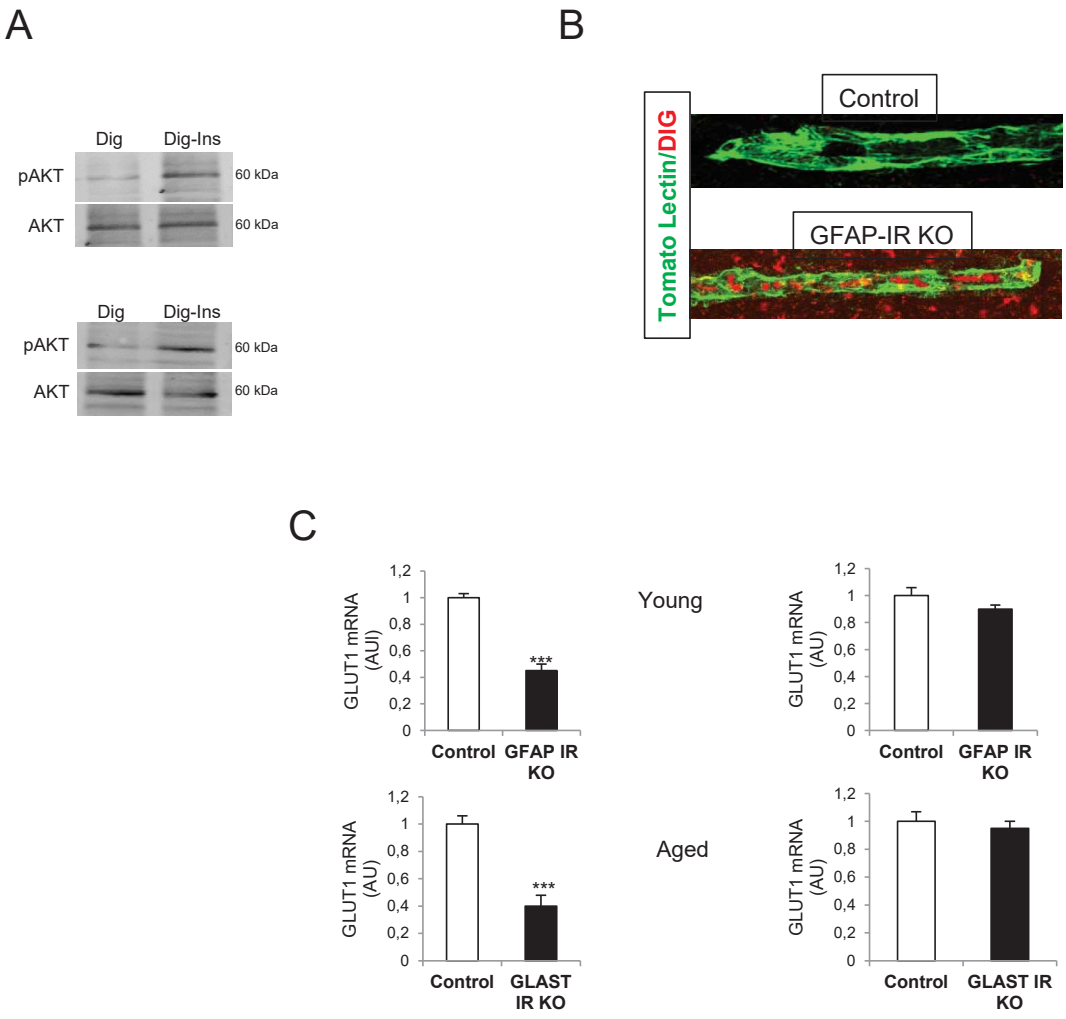
A
Dig
Dig-Ins
pAKT
AKT
60 kDa
60 kDa
Dig
Dig-Ins
pAKT
AKT
60 kDa
60 kDa
B
Control
GFAP-IR KO
Tomato Lectin/DIG
C
GLUT1 mRNA (AUI)
1,2
1
0,8
0,6
0,4
0,2
0
***
Control
GFAP IR KO
Young
GLUT1 mRNA (AU)
Control
GFAP IR KO
GLUT1 mRNA (AU)
***
Control
GLAST IR KO
Aged
GLUT1 mRNA (AU)
Control
GLAST IR KO

Figure S2

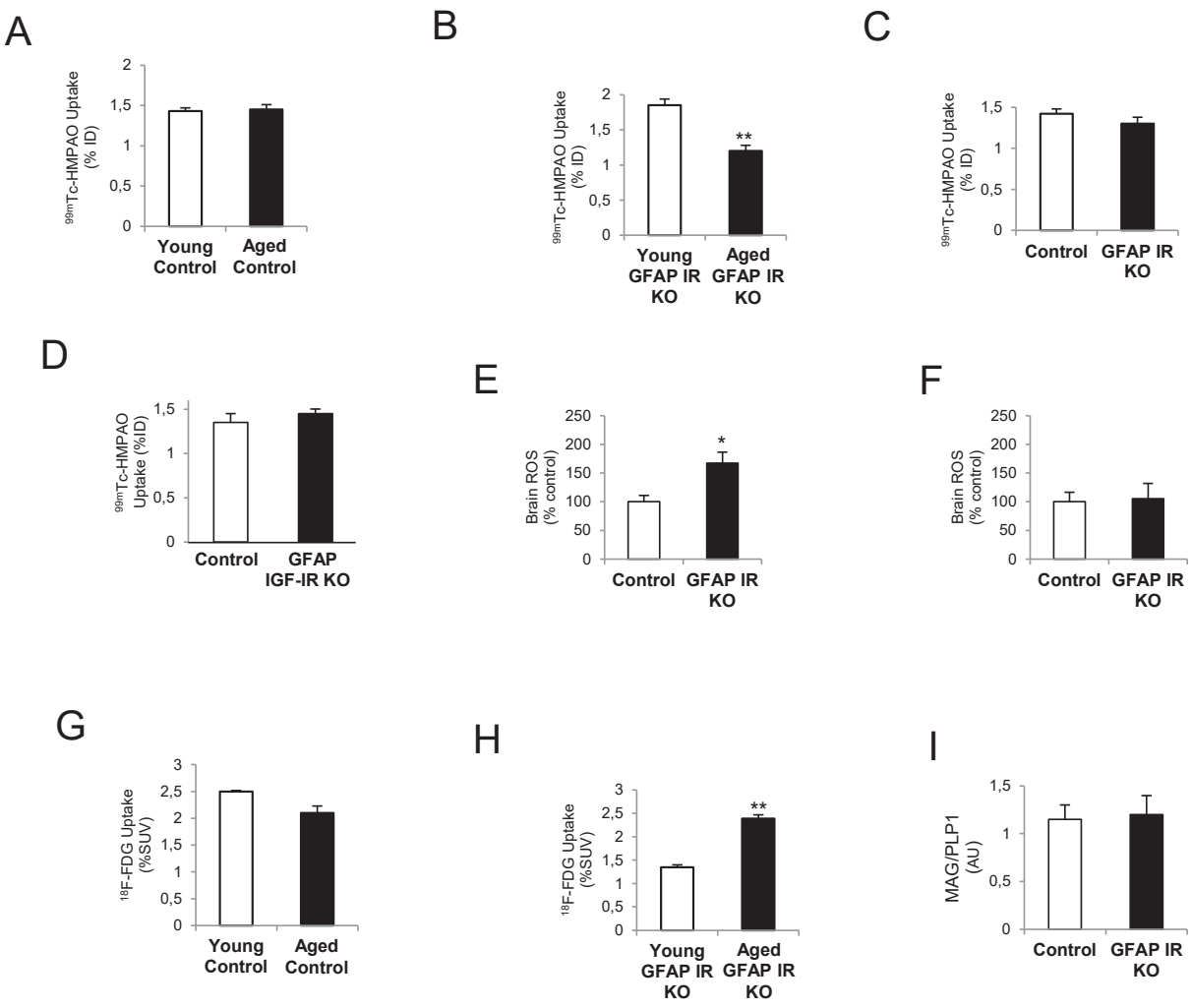
A
99mTc-HMPAO Uptake (% ID)
2
1,5
1
0,5
0
Young Control
Aged Control
B
99mTc-HMPAO Uptake (% ID)
2
1,5
1
0,5
0
**
Young GFAP IR KO
Aged GFAP IR KO
C
99mTc-HMPAO Uptake (% ID)
1,5
1
0,5
0
Control
GFAP IR KO
D
99mTc-HMPAO Uptake (%ID)
1,5
1
0,5
0
Control
GFAP IGF-IR KO
E
Brain ROS (% control)
250
200
150
100
50
0
*
Control
GFAP IR KO
F
Brain ROS (% control)
250
200
150
100
50
0
Control
GFAP IR KO
G
18F-FDG Uptake (%SUV)
3
2,5
2
1,5
1
0,5
0
Young Control
Aged Control
H
18F-FDG Uptake (%SUV)
3
2,5
2
1,5
1
0,5
0
**
Young GFAP IR KO
Aged GFAP IR KO
I
MAG/PLP1 (AU)
1,5
1
0,5
0
Control
GFAP IR KO

Figure S3

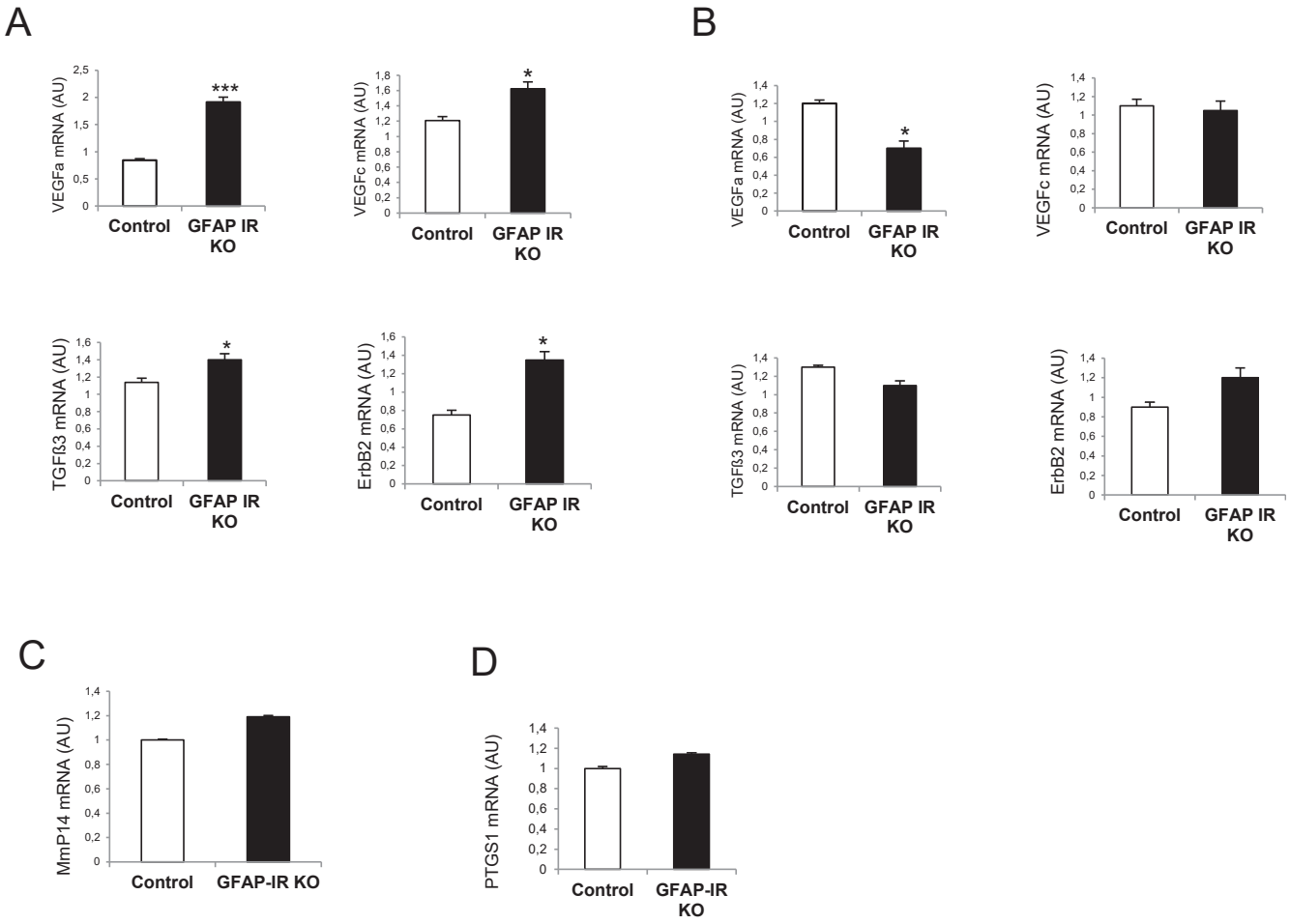
A
VEGFa mRNA (AU)
***
Control
GFAP IR KO
VEGFc mRNA (AU)
*
Control
GFAP IR KO
TGFß3 mRNA (AU)
*
Control
GFAP IR KO
ErbB2 mRNA (AU)
*
Control
GFAP IR KO
B
VEGFa mRNA (AU)
*
Control
GFAP IR KO
VEGFc mRNA (AU)
Control
GFAP IR KO
TGFß3 mRNA (AU)
Control
GFAP IR KO
ErbB2 mRNA (AU)
Control
GFAP IR KO
C
MmP14 mRNA (AU)
Control
GFAP-IR KO
D
PTGS1 mRNA (AU)
Control
GFAP-IR KO

Figure S4

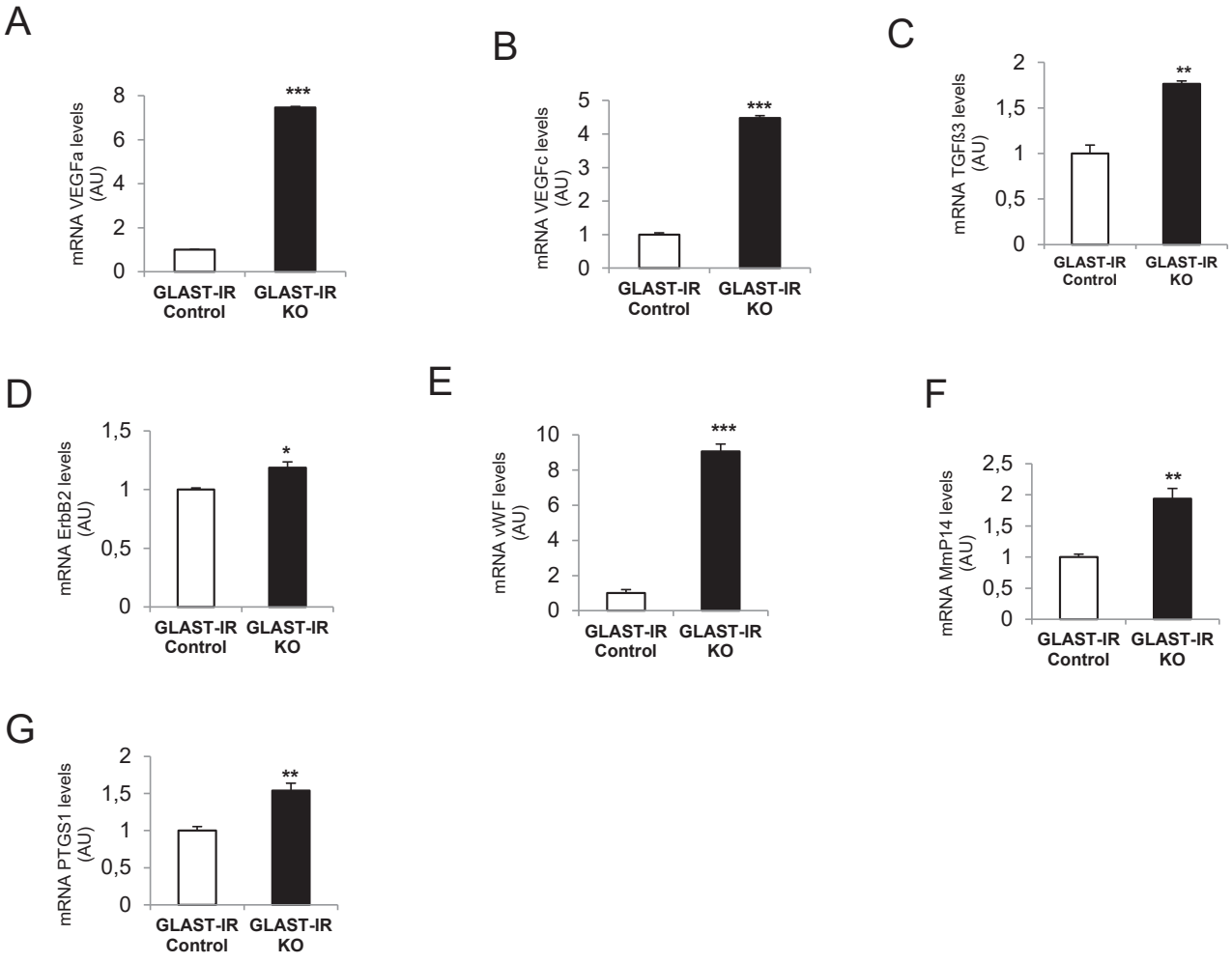
A
mRNA VEGFa levels (AU)
8
6
4
2
0
***
GLAST-IR Control
GLAST-IR KO
B
mRNA VEGFc levels (AU)
5
4
3
2
1
0
***
GLAST-IR Control
GLAST-IR KO
C
mRNA TGFß3 levels (AU)
2
1,5
1
0,5
0
**
GLAST-IR Control
GLAST-IR KO
D
mRNA ErbB2 levels (AU)
1,5
1
0,5
0
*
GLAST-IR Control
GLAST-IR KO
E
mRNA vWF levels (AU)
10
8
6
4
2
0
***
GLAST-IR Control
GLAST-IR KO
F
mRNA MmP14 levels (AU)
2,5
2
1,5
1
0,5
0
**
GLAST-IR Control
GLAST-IR KO
G
mRNA PTGS1 levels (AU)
2
1,5
1
0,5
0
**
GLAST-IR Control
GLAST-IR KO

Figure S5

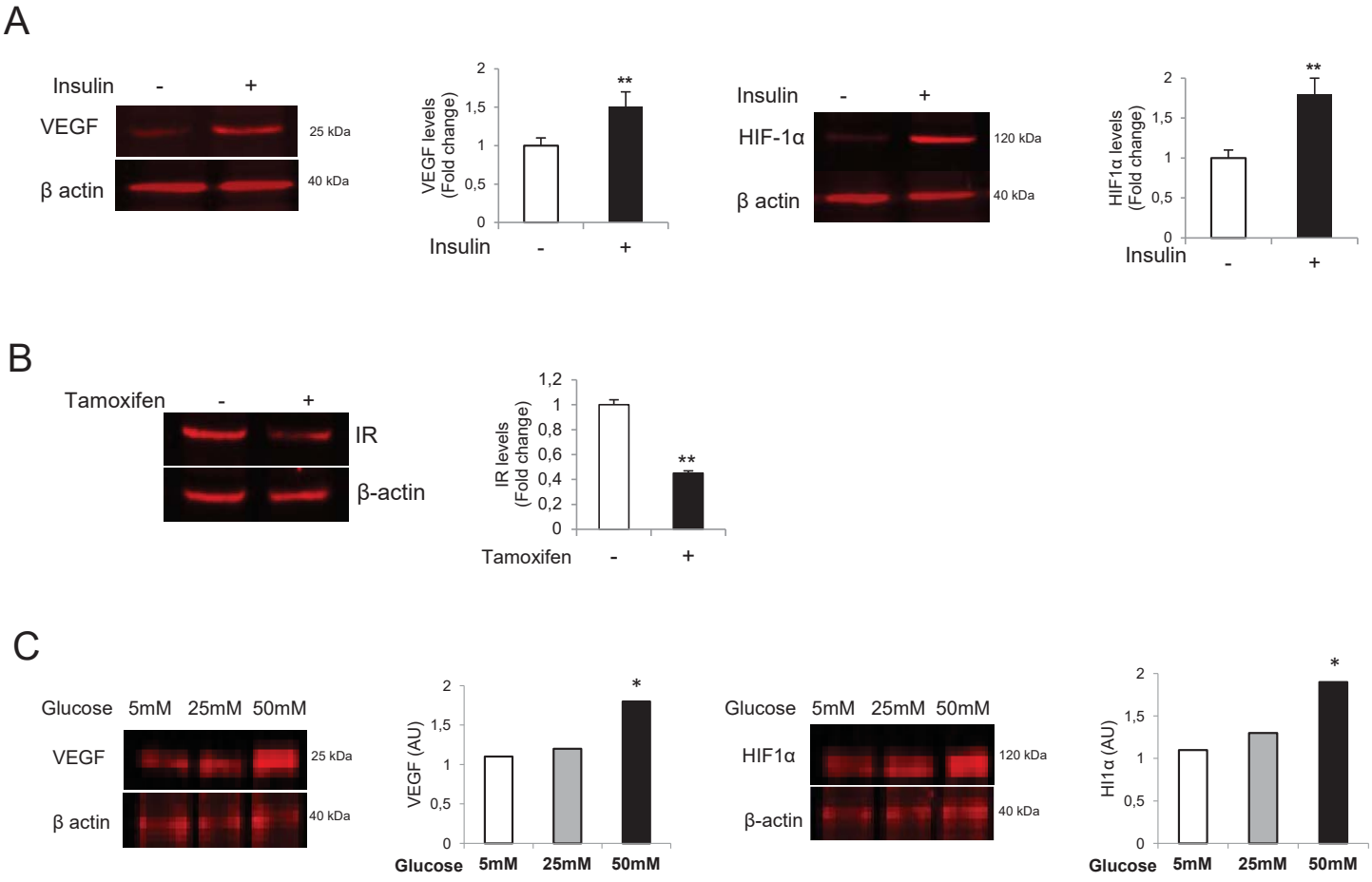
A
Insulin - +
VEGF
β actin
25 kDa
40 kDa
VEGF levels (Fold change)
2
1,5
1
0,5
0
**
Insulin - +
Insulin - +
HIF-1α
β actin
120 kDa
40 kDa
HIF1α levels (Fold change)
2
1,5
1
0,5
0
**
Insulin - +
B
Tamoxifen - +
IR
β-actin
IR levels (Fold change)
1,2
1
0,8
0,6
0,4
0,2
0
**
Tamoxifen - +
C
Glucose 5mM 25mM 50mM
VEGF
β actin
25 kDa
40 kDa
VEGF (AU)
2
1,5
1
0,5
0
*
Glucose 5mM 25mM 50mM
Glucose 5mM 25mM 50mM
HIF1α
β-actin
120 kDa
40 kDa
HI1α (AU)
2
1,5
1
0,5
0
*
Glucose 5mM 25mM 50mM

Figure S6

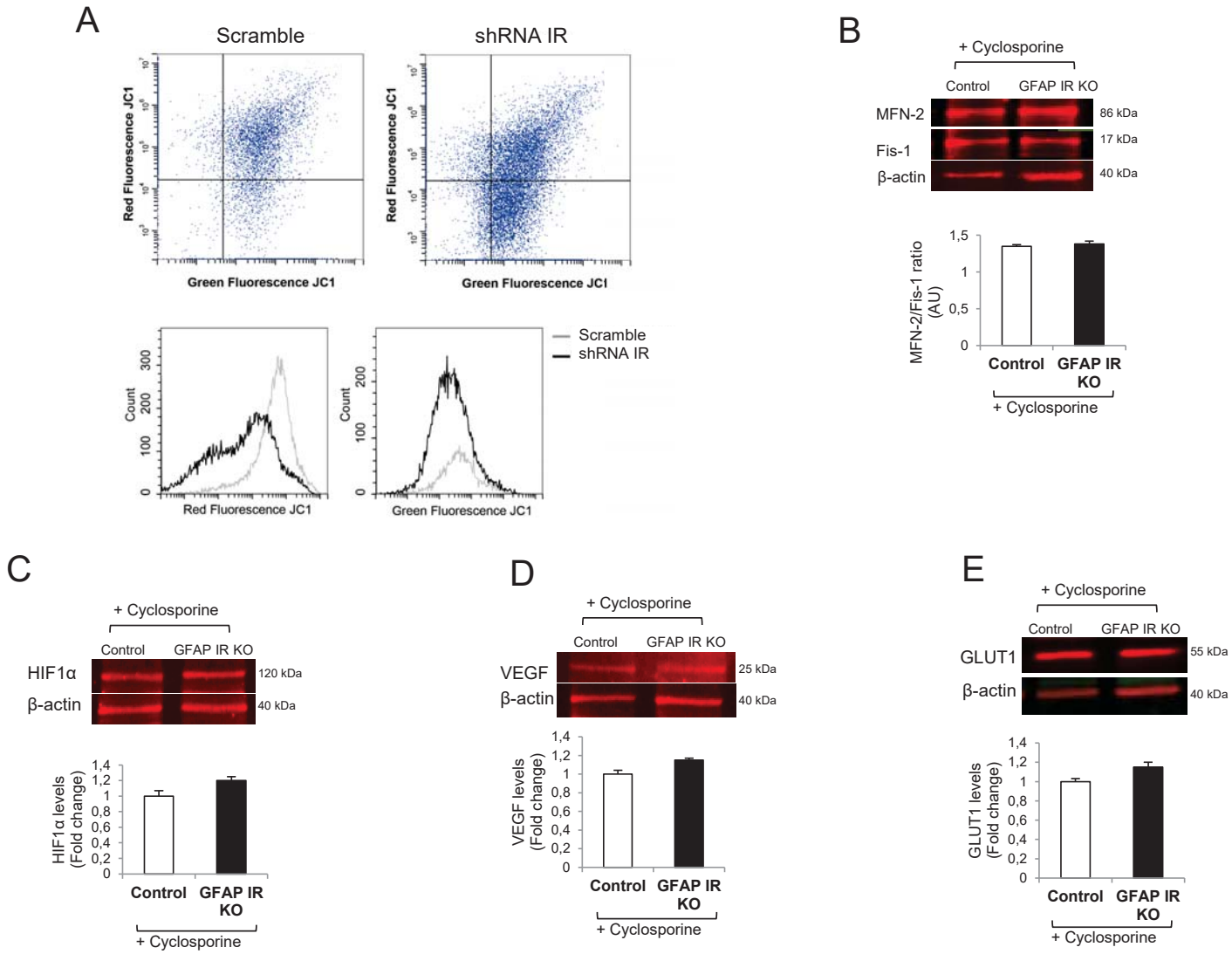
A
Scramble
shRNA IR
Red Fluorescence JC1
Green Fluorescence JC1
Count
Scramble
shRNA IR
B
+ Cyclosporine
Control
GFAP IR KO
MFN-2
Fis-1
β-actin
86 kDa
17 kDa
40 kDa
MFN-2/Fis-1 ratio (AU)
C
HIF1α
120 kDa
HIF1α levels (Fold change)
D
VEGF
25 kDa
VEGF levels (Fold change)
E
GLUT1
55 kDa
GLUT1 levels (Fold change)

Figure S7

SI References

1. Garcia-Caceres, C., Quarta, C., Varela, L., Gao, Y., Gruber, T., Legutko, B., Jastroch, M., Johansson, P., Ninkovic, J., Yi, C.X., et al. (2016). Astrocytic Insulin Signaling Couples Brain Glucose Uptake with Nutrient Availability. Cell*166*, 867-880. 10.1016/j.cell.2016.07.028.
2. Ganat, Y.M., Silbereis, J., Cave, C., Ngu, H., Anderson, G.M., Ohkubo, Y., Ment, L.R., and Vaccarino, F.M. (2006). Early postnatal astroglial cells producemultilineage precursors and neural stem cells in vivo. J Neurosci *26*, 8609-8621.10.1523/JNEUROSCI.2532-06.2006.
3. Fernandez, A.M., Hernandez-Garzon, E., Perez-Domper, P., Perez-Alvarez, A., Mederos, S., Matsui, T., Santi, A., Trueba-Saiz, A., Garcia-Guerra, L., Pose-Utrilla, J., et al. (2017). Insulin Regulates Astrocytic Glucose Handling ThroughCooperation With IGF-I. Diabetes *66*, 64-74. 10.2337/db16-0861.
4. Perriere, N., Demeuse, P., Garcia, E., Regina, A., Debray, M., Andreux, J.P., Couvreur, P., Scherrmann, J.M., Temsamani, J., Couraud, P.O., et al. (2005). Puromycin-based purification of rat brain capillary endothelial cell cultures. Effect on the expression of blood-brain barrier-specific properties. J Neurochem*93*, 279-289.
5. Munive, V., Zegarra-Valdivia, J.A., Herrero-Labrador, R., Fernandez, A.M., andAleman, I.T. (2019). Loss of the interaction between estradiol and insulin-like growth factor I in brain endothelial cells associates to changes in mood homeostasis during peri-menopause in mice. Aging (Albany NY) *11*, 174-184. 10.18632/aging.101739.
6. Fernandez, A.M., Jimenez, S., Mecha, M., Davila, D., Guaza, C., Vitorica, J.,and Torres-Aleman, I. (2012). Regulation of the phosphatase calcineurin by insulin-like growth factor I unveils a key role of astrocytes in Alzheimer's pathology. Mol Psychiatry *17*, 705-718.
7. Martinez-Rachadell, L., Aguilera, A., Perez-Domper, P., Pignatelli, J., Fernandez, A.M., and Torres-Aleman, I. (2019). Cell-specific expression of insulin/insulin-like growth factor-I receptor hybrids in the mouse brain. GrowthHorm IGF Res *45*, 25-30. 10.1016/j.ghir.2019.02.003.

8. Fernandez de Sevilla, M.E., Pignatelli, J., Zegarra-Valdivia, J.A., Mendez, P., Nunez, A., and Torres Aleman, I. (2022). Insulin-like growth factor I mitigatespost-traumatic stress by inhibiting AMP-kinase in orexin neurons. Mol Psychiatry. 10.1038/s41380-022-01442-9.

9. Fernandez, A.M., Fernandez, S., Carrero, P., Garcia-Garcia, M., and Torres-Aleman, I. (2007). Calcineurin in reactive astrocytes plays a key role in the interplay between proinflammatory and anti-inflammatory signals. J Neurosci*27*, 8745-8756.

10. Gomez-Arboledas, A., Davila, J.C., Sanchez-Mejias, E., Navarro, V., Nunez-Diaz, C., Sanchez-Varo, R., Sanchez-Mico, M.V., Trujillo-Estrada, L., Fernandez-Valenzuela, J.J., Vizuete, M., et al. (2018). Phagocytic clearance ofpresynaptic dystrophies by reactive astrocytes in Alzheimer's disease. Glia *66*,637-653. 10.1002/glia.23270.

11. Hernandez-Garzon, E., Fernandez, A.M., Perez-Alvarez, A., Genis, L., Bascunana, P., Fernandez de la Rosa, R., Delgado, M., Angel Pozo, M., Moreno,E., McCormick, P.J., et al. (2016). The insulin-like growth factor I receptor regulates glucose transport by astrocytes. Glia *64*, 1962-1971. 10.1002/glia.23035.

12. Behrens, M.M., Ali, S.S., Dao, D.N., Lucero, J., Shekhtman, G., Quick, K.L.,and Dugan, L.L. (2007). Ketamine-induced loss of phenotype of fast-spiking interneurons is mediated by NADPH-oxidase. Science *318*, 1645-1647. 10.1126/science.1148045.

13. Davila, D., and Torres-Aleman, I. (2008). Neuronal Death by Oxidative Stress Involves Activation of FOXO3 through a Two-Arm Pathway That Activates Stress Kinases and Attenuates Insulin-like Growth Factor I Signaling. MolecularBiology of the Cell *19*, 2014-2025.